Waveform Characterization of Microwave Power Heterojunction Bipolar Transistors

C. J. Wei, Y. Lan and J. C. M. Hwang
Lehigh University, 19 Memorial Dr W, Bethlehem PA 18015

W. J. Ho and J. A. Higgins
Rockwell International, 1049 Camino Dos Rios, Thousand Oaks, CA 91360

Abstract—Time-domain waveform characterization has been successfully applied to microwave power heterojunction bipolar transistors, for extraction and verification of their large-signal nonlinear characteristics. Compared to the conventional dc and small-signal techniques, this new technique is inherently more accurate and allows insight into the transistor operation.

Large-signal transistor characterization based on dc *I-V* characteristics and frequency-domain *S*-parameters is often confronted with the inconsistency between these two sets of data due to various time-dependent phenomena. In comparison, time-domain waveform characterization literally allows insight into transistor nonlinearity without ambiguity [1]-[4]. [1]-[4] pertain to MESFETs only. This paper reports the first waveform characterization of the intrinsic characteristics of microwave power HBTs.

These HBTs are of the *npn* GaAs/AlGaAs variety having a total emitter area of approximately 300 μm^2. Under the bias conditions used in this study, the current-gain cutoff frequency and the maximum frequency of oscillation is in the range of 30 to 40 GHz. The details of the HBTs have been described elsewhere [5].

The HBTs are characterized on-wafer using a pair of GGB 40A probes as shown schematically in Fig. 1. The HBT is driven at 2 GHz from 8 to 12 dBm. Since the primary purpose of this study is to demonstrate the characterization technique, the maximum input drive level is approximately 3 dB backed off from saturation. Two directional couplers are used on the input side for measuring the incident and reflected waves. The waves at Port 3, 4 and 6, including up to their seventh harmonics, are measured by a HP 70820A Transition Analyzer. Having individually characterized the probes, couplers and bias-T's, the measured waveforms can be transformed to Port 2 and 5, at the HBT input and output, respectively (Fig. 2).

$$a2 = \frac{S31\ b4 - S41\ b3}{S31\ S42 - S32\ S41} \tag{1}$$

$$b2 = S22\ a2 + S21\ \frac{S42\ b3 - S32\ b4}{S31\ S42 - S32\ S41} \tag{2}$$

$$a5 = \frac{b6}{S65} \tag{3}$$

$$b5 = S55\ a5 \tag{4}$$

Next, to gain insight into the HBT intrinsic characteristics, the waveforms at Port 2 and 5 are transformed to the HBT internal nodes, b', e' and c', as depicted in Fig. 3. Here the extrinsic parameters of the equivalent circuit have been extracted from bias-dependent *S*-parameters according to a previously reported method [6]. From the internal waveforms, the intrinsic HBT parameters, which are all highly nonlinear, can be extracted.

Figure 4 shows the HBT external waveforms,

TH 3B

CH3577-4/95/0000-1239$01.00 © 1995 IEEE

Vc, *Vb*, *Ic* and *Ib*, measured under Class C bias (*Vce* = 4 V; *Vbe* = 0.8 V) and 11 dBm input drive. To visualize how these waveforms are related to each other, Fig. 5 and 6 depict the RF contours at the external base and collector ports, respectively, for various input levels. It can be seen that the base contours contain a large loop, indicating that the displacement current dominates the conduction current due to the extrinsic capacitances. In comparison, the collector contours are greatly elongated, reflecting the 50 Ω load.

Figure 7 and 8 are intrinsic contours of *Ie*(*Vb'e'*) and *Ic'*(*Ie*). Notice that *Ie'* = *Ie* which is the actual current across the intrinsic base-emitter junction. From Fig. 7 this current is dominated by diode-like conduction above 1.3 V, and, only a small capacitance is present below 1.3 V. The intrinsic base-emitter diode characteristics are then fitted to a two-term Ebers-Moll exponential function. Similarly, the charge storage characteristics are expressed in terms of diffusion capacitance and space charge. It turns out that the diffusion capacitance is much smaller than the space charge, perhaps due to ballistic transport of the electrons across the base. Figure 9 shows that the modeled and measured intrinsic base-emitter characteristics are in reasonable agreement. Figure 10 illustrates the fitting of the intrinsic collector current as a function of the emitter current. Here a Gummel-Poon model with a constant delay time is used. The fitted parameter values (Table I) are all physically reasonable and they represent an improvement over those extracted from *S*-parameters.

In conclusion, time-domain waveform characterization has been successfully applied to microwave power HBTs to extract their nonlinear characteristics. This new characterization technique is inherently more direct and accurate. It literally allows insight into the HBT operation based on which the circuit application of the HBT can be optimized.

REFERENCES

[1] F. N. Sechi, H. C. Huang and B. S. Perlman, "Voltage and current waveforms in power MESFETs at microwave frequencies," in *Dig. Int'l Solid-state Circuits Conf.*, 1978, pp. 168-169.

[2] F. van Raay and G. Kompa, "A new on-wafer large-signal waveform measurement system with 40 GHz harmonic bandwidth," in *IEEE MTT-S Int'l Microwave Symp. Dig.*, 1992, pp. 1435-1438.

[3] C. J. Wei, Y. A. Tkachenko and J. C. M. Hwang, "Non-invasive waveform probing for nonlinear network analysis," in *IEEE MTT-S Int'l Microwave Symp. Dig.*, 1993, pp. 1347-1350.

[4] A. Werthof, F. van Raay and G. Kompa, "Direct nonlinear FET parameter extraction using large-signal waveform measurements," *IEEE Microwave and Guided Wave Letters*, vol. 3, no. 5, 1993, pp. 130-132.

[5] W. J. Ho, N. L. Wang, M. F. Chang and J. A. Higgins, "Producibility and performance of the microwave power HBT," in *IEEE GaAs IC Symp. Technical Dig.*, 1992, pp. 263-266.

[6] C. J. Wei and J. C. M. Hwang, "New method for direct extraction of HBT equivalent circuit parameters,", in *IEEE MTT-S Int'l Microwave Symp. Dig.*, 1994, pp. 1245-1248.

TABLE I
INTRINSIC HBT MODEL PARAMETERS

Emitter Conduction Current	Emitter Displacement Current	Collector Conduction Current
$I0=1.7\times10^{-19}$ A	$C0=0.44$ pF	$\alpha0=0.986$
$n=1.52$	$Vbi=1.98$ V	$Ikf=0.87$ A
$Ie0=2.23\times10^{-14}$ A	$\tau b=0.1$ ps	$\tau c=5.3$ ps
$ne=2.02$		

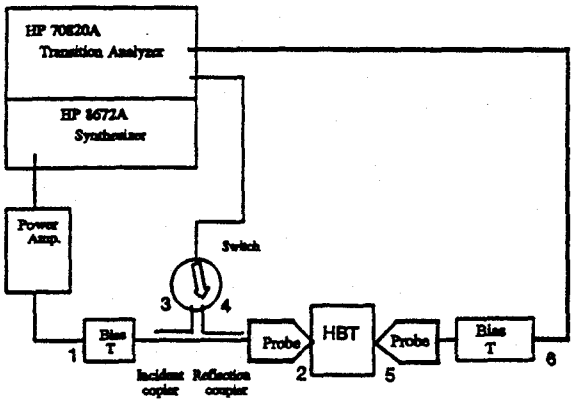

Fig. 1 Schematics of the waveform measurement setup.

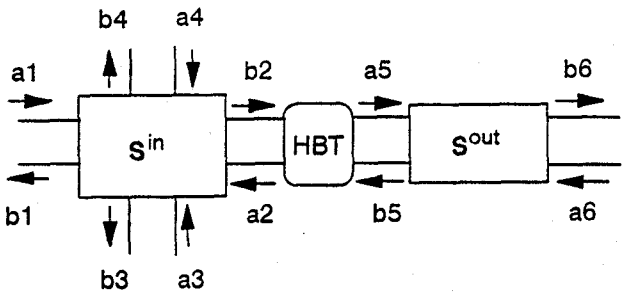

Fig. 2 *S*-parameter representation of the measurement setup.

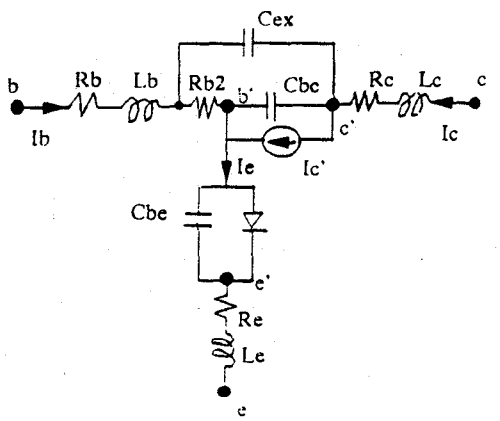

Fig. 3 HBT hybrid-T equivalent circuit.

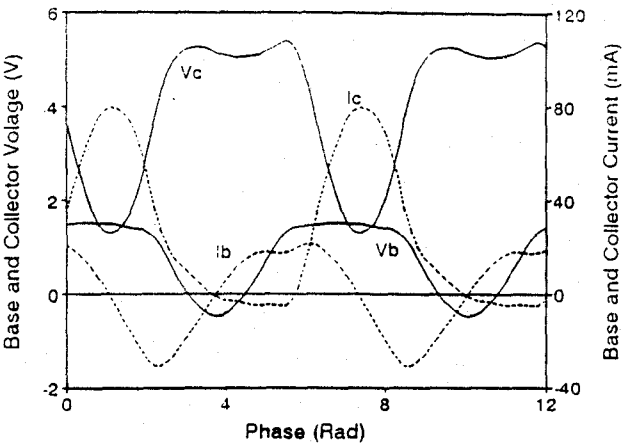

Fig. 4 Measured extrinsic base and collector waveforms, under a 2 GHz, 11 dBm input drive.

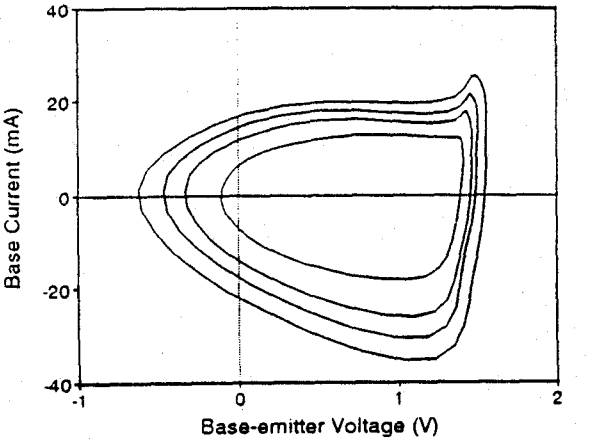

Fig. 5 Measured extrinsic base current vs. base-emitter voltage. The input power is varied from 8, 10, 11, to 12 dBm.

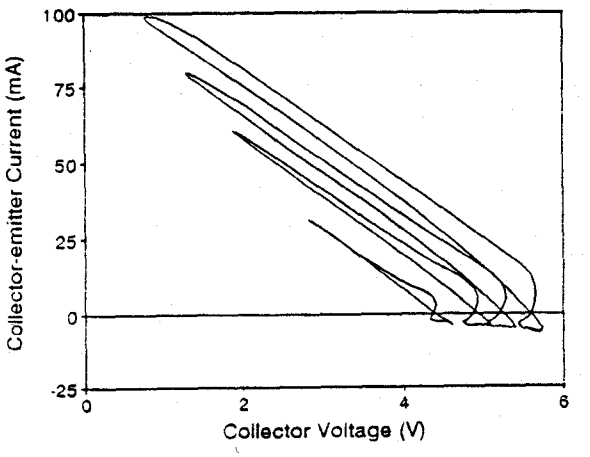

Fig. 6 Measured extrinsic collector current vs. collector-emitter voltage. The input power is varied from 8, 10, 11, to 12 dBm.

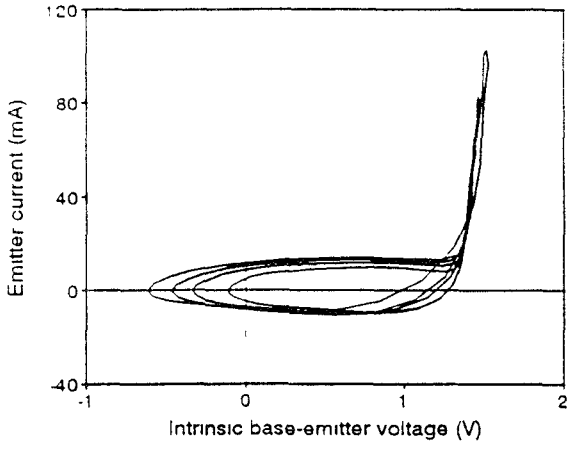

Fig. 7 Measured intrinsic emitter current vs. base-emitter voltage. The input power is varied from 8, 10, 11, to 12 dBm.

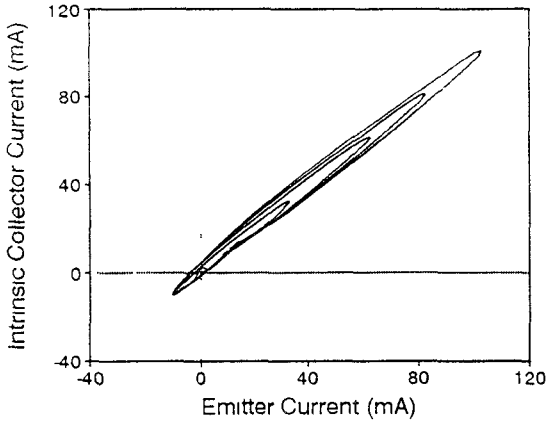

Fig. 10 Modeled intrinsic collector current vs. emitter current. The input power is varied from 8, 10, 11, to 12 dBm.

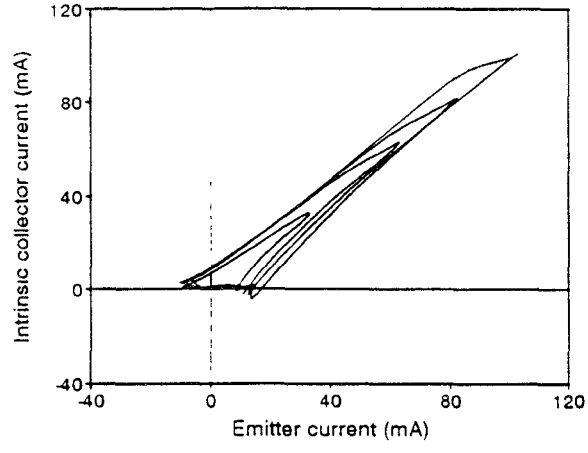

Fig. 8 Measured intrinsic collector current vs. emitter current. The input power is varied from 8, 10, 11, to 12 dBm.

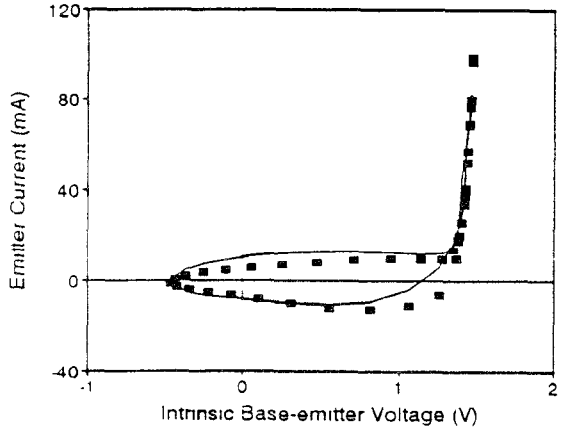

Fig. 9 (—) modeled vs. (■) measured emitter current, for an input power of 11 dBm.